

# A Microfluidic Platform Using Molecular Beacon-Based Temperature Calibration for Thermal Dehybridization of Surface-Bound DNA

Arash Dodge, Gerardo Turcatti,<sup>\*,†,§</sup> Isabelle Lawrence,<sup>§</sup> Nico F. de Rooij, and Elisabeth Verpoorte<sup>\*,‡</sup>

Sensors, Actuators and Microsystems Laboratory, Institute of Microtechnology, University of Neuchâtel, Rue Jaquet-Droz 1, CH-2007 Neuchâtel, Switzerland, and Manteia SA, Zone industrielle, CH-1267 Coinsins, Switzerland

**This work presents a simple microfluidic device with an integrated thin-film heater for studies of DNA hybridization kinetics and double-stranded DNA melting temperature measurements. The heating characteristics of the device were evaluated with a novel, noninvasive indirect technique using molecular beacons as temperature probes inside reaction chambers. This is the first microfluidic device in which thermal dehybridization of surface-bound oligonucleotides was performed for measurement of double-stranded DNA melting temperatures with  $\pm 1$  °C precision. Surface modification and oligonucleotide immobilization were performed by continuously flowing reagents through the microchannels. The resulting reproducibility of oligonucleotide surface densities, at 9% RSD, was better than for the same modification chemistries on glass slides in unstirred reagent solutions (RSD = 20%). Moreover, the surface density of immobilized DNA probe molecules could be varied controllably by changing the concentration of the reagent solution used for immobilization. Thus, excellent control of surface characteristics was made possible, something which is often difficult to achieve with larger devices. Solid-phase hybridization reactions, a fundamental aspect of microarray technologies often taking several hours in conventional systems, were reduced to minutes in this device. It was also possible to determine forward rate constants for hybridization,  $k$ . These varied from 820 000 to 72 000 M<sup>-1</sup> s<sup>-1</sup>, decreasing as surface densities increased. Surface densities could therefore be optimized to obtain rapid hybridization using such an approach. Taken together, this combined microfluidic/small-volume heating approach represents a powerful tool for surface-based DNA analysis.**

With the huge increase in DNA sequence information resulting from the Human Genome Project, genetics researchers are now focusing on establishing the link between sequence and function.

In pharmacogenomics, for instance, the relationship between DNA sequence composition and drug response is of particular interest, as pharmaceutical companies seek to better design medicines to avoid adverse side effects and generally improve drug therapies. Medical diagnostics has also benefited enormously, as more and more tests for inherited diseases rely on testing patient DNA for characteristic mutations by hybridization with DNA probes of known sequence. An integral part of genetics research today involves the discovery of single-nucleotide polymorphisms (SNPs), single-base variations which could potentially play a large role in determining phenotype. Traditionally, DNA analysis has been performed with instruments based on gel electrophoresis, which separate DNA fragments according to size. This method is difficult to perform with high throughput, since analysis times are in the order of hours. Microfluidic chips have provided a way to downsize this technology, strongly reducing analysis times while maintaining or exceeding the separation efficiencies achieved in macroscopic instruments.<sup>1–6</sup> Multiplexing DNA analysis also becomes possible simply by reproducing the channel layout many times to form an array of closely spaced separation channels for highly parallel, high-throughput analysis.<sup>7–14</sup>

- (1) Effenhauser, C. S.; Paulus, A.; Manz, A.; Widmer, H. M. *Anal. Chem.* **1994**, *66*, 2949–2953.
- (2) Schmalzing, D.; Adourian, A.; Koutny, L.; Ziaugra, L.; Matsudaira, P.; Ehrlich, D. *Anal. Chem.* **1998**, *70*, 2303–2310.
- (3) Liu, S. R.; Shi, Y. N.; Ja, W. W.; Mathies, R. A. *Anal. Chem.* **1999**, *71*, 566–573.
- (4) Shi, Y. N.; Simpson, P. C.; Scherer, J. R.; Wexler, D.; Skibola, C.; Smith, M. T.; Mathies, R. A. *Anal. Chem.* **1999**, *71*, 5354–5361.
- (5) Munro, N. J.; Snow, K.; Kant, J. A.; Landers, J. P. *Clin. Chem.* **1999**, *45*, 1906–1917.
- (6) Schmalzing, D.; Koutny, L.; Chisholm, D.; Adourian, A.; Matsudaira, P.; Ehrlich, D. *Anal. Biochem.* **1999**, *270*, 148–52.
- (7) Simpson, P. C.; Roach, D.; Woolley, A. T.; Thorsen, T.; Johnston, R.; Sensabaugh, G. F.; Mathies, R. A. *Proc. Natl. Acad. Sci. U.S.A.* **1998**, *95*, 2256–2261.
- (8) Huang, Z.; Munro, N.; Huhmer, A. F. R.; Landers, J. P. *Anal. Chem.* **1999**, *71*, 5309–5314.
- (9) Medintz, I.; Wong, W. W.; Sensabaugh, G.; Mathies, R. A. *Electrophoresis* **2000**, *21*, 2352–2358.
- (10) Sassi, A. P.; Paulus, A.; Cruzado, I. D.; Bjornson, T.; Hooper, H. H. J. *Chromatogr., A* **2000**, *894*, 203–217.
- (11) Medintz, I. L.; Berti, L.; Emrich, C. A.; Tom, J.; Scherer, J. R.; Mathies, R. A. *Clin. Chem.* **2001**, *47*, 1614–21.
- (12) Medintz, I.; Wong, W. W.; Berti, L.; Shio, L.; Tom, J.; Scherer, J.; Sensabaugh, G.; Mathies, R. A. *Genome Res.* **2001**, *11*, 413–421.
- (13) Emrich, C. A.; Tian, H. J.; Medintz, I. L.; Mathies, R. A. *Anal. Chem.* **2002**, *74*, 5076–5083.

\* Address correspondence to either author.

<sup>†</sup> Phone: +41 22 354 58 01. Fax: +41 22 995 01 50. E-mail: gerardo.turcatti.com.

<sup>‡</sup> Current address: Groningen Research Institute of Pharmacy, University of Groningen, Antonius Deusinglaan 1, P.O. Box 196, 9700 AD Groningen, The Netherlands. Phone: +31 50 363 33 37. Fax: + 31 50 363 75 82. E-mail: S.Verpoorte@farm.rug.nl.

<sup>§</sup> Manteia S.A.

An alternative approach to high-throughput DNA analysis is offered by DNA microarray-based chips, involving the synthesis or immobilization of many thousands of probe oligomers onto a surface as arrays of spots. Analysis is then performed by introducing the target DNA to the liquid volume above the array and allowing hybridization to occur. Detection is generally accomplished by fluorescently labeling the target DNA beforehand so that hybridization leads to an increase in optical signal. There is no doubt that this technology has revolutionized genetics research. However, besides the nonnegligible cost of the probes and spotting instrumentation, analysis time is still a concern. This is because chip-based hybridization assays still generally depend solely on diffusion of target (sample) DNA to the surface-bound probes, leading to hybridization times of several hours or more.<sup>15–17</sup> To address this problem, DNA array chips have been combined with microfluidic devices designed to mix and circulate hybridization sample over the array surface to enhance sensitivity and, thus, provide a route to reduced hybridization times.<sup>16,18</sup> Alternatively, probe DNA has been spotted directly into a polycarbonate microchannel. An integrated pump was then used to accelerate hybridization by moving sample through the channel.<sup>15</sup> Detection could be carried out in only 30 min. Other solid-phase hybridization-based analysis methods have used either novel solid phases or DNA transport to achieve improved performance. Improved interaction with surface-immobilized DNA by reducing diffusional transport distances was also achieved by depositing spots of probe-containing solution on microchannel glass, a porous substrate consisting of vertical microchannels 10  $\mu\text{m}$  in diameter.<sup>17,19</sup> Recirculation of target-containing sample through the substrate guaranteed efficient delivery of target to the surface. DNA has also been immobilized in porous hydrogel plugs in microfluidic channels. Electrophoretic perfusion of the plugs with complementary DNA allowed hybridization to take place in minutes.<sup>20</sup> These examples demonstrate that active delivery of hybridization solutions or DNA molecules directly to DNA-probe-coated surfaces strongly enhances the rate of hybridization and the sensitivity of the resulting signal when compared to systems in which transport is solely passive.

Surface chemistry combined with heat can be a powerful tool for DNA analysis. One recent report described an example of SNP analysis performed by thermal dehybridization of surface-bound DNA in a technique known as *dynamic allele-specific hybridization* (DASH).<sup>21,22</sup> Target DNA is immobilized after amplification to a

microtiter plate well using biotin–streptavidin chemistry and hybridized with a probe specific for one allele. Hybridization is visualized using a double-stranded DNA-specific dye. Monitoring fluorescence as temperature is ramped should then yield a rapid decrease in fluorescence at the denaturing or “melting” temperature,  $T_m$ , of the target-probe duplex.  $T_m$ 's were lower for sequences containing a SNP than for fully hybridized strands, with temperature differences on the order of 6–12 °C for 15- to 21-mer probes.<sup>21–23</sup> Thiel et al. observed similar values for in situ surface plasmon resonance imaging of DNA hybridization at gold surfaces.<sup>24</sup>

To perform the type of DNA analysis described above on a microfluidic platform, one has to address the issues of sample delivery and small-volume liquid handling generally, as well as temperature control and surface modification in microchannels. The large surface-to-volume ratios characteristic of microfluidic devices provide for efficient heat transport and, thus, greater temperature uniformity and control. This aspect was important in this study, as it was of interest to monitor thermal dehybridization in microchannels through integration of a thin-film heater, as proposed by a number of authors for microchip-based PCR.<sup>25–29</sup> To characterize a device with respect to temperature, a thermocouple may be inserted directly into a reaction chamber in order to perform temperature measurements in a straightforward way.<sup>30,31</sup> However, the presence of a foreign body in the small cavity could affect temperature uniformity or inhibit certain types of biochemical reactions. Therefore, efforts by a number of groups to integrate resistive temperature sensing electrodes directly into devices in order to enhance speed of analysis have been reported.<sup>25–27,32–34</sup> Backscatter interferometry has also been developed as an indirect noninvasive method in order to measure temperature inside a chamber.<sup>35</sup> Alternatively, the use of thermochromic liquid crystals has been reported.<sup>36</sup> We propose a novel, noninvasive way of calibrating temperature inside a microchannel using molecular beacons as temperature probes.

Molecular beacons are molecules that have recently been developed in order to recognize and report the presence of specific

(14) Paegel, B. M.; Emrich, C. A.; Weyemayer, G. J.; Scherer, J. R.; Mathies, R. A. *Proc. Natl. Acad. Sci. U.S.A.* **2002**, *99*, 574–579.  
 (15) Lenigk, R.; Liu, R. H.; Athavale, M.; Chen, Z.; Ganser, D.; Yang, J.; Rauch, C.; Liu, Y.; Chan, B.; Yu, H.; Ray, M.; Marrero, R.; Grodzinski, P. *Anal. Biochem.* **2002**, *311*, 40–49.  
 (16) Yuen, P. K.; Li, G.; Bao, Y.; Müller, U. R. *Lab Chip* **2003**, *3*, 46–50.  
 (17) Schena, M. *Microarray Biochip Technology*; Eaton Publishing: Sunnyvale, CA, 2000; pp 87–187.  
 (18) Adey, N. B.; Lei, M.; Howard, M. T.; Jensen, J. D.; Mayo, D. A.; Butel, D. L.; Coffin, S. C.; Moyer, T. C.; Slade, D. E.; Spute, M. K.; Hancock, A. M.; Eisenhoffer, G. T.; Dalley, B. K.; McNeely, M. R. *Anal. Chem.* **2002**, *74*, 6413–6417.  
 (19) Cheek, B. J.; Steel, A. B.; Torres, M. P.; Yu, Y.-Y.; Yang, H. *Anal. Chem.* **2001**, *73*, 5777–5783.  
 (20) Olsen, K. G.; Ross, D. J.; Tarlov, M. J. *Anal. Chem.* **2002**, *74*, 1436–1441.  
 (21) Howell, W. M.; Jobs, M.; Gyllensten, U.; Brookes, A. J. *Nat. Biotechnol.* **1999**, *17*, 87–88.  
 (22) Prince, J. A.; Feuk, L.; Howell, W. M.; Jobs, M.; Emahazion, T.; Blennow, K.; Brookes, A. J. *Genome Res.* **2001**, *11*, 152–162.

(23) Jobs, M.; Fredriksson, S.; Brookes, A. J.; Landegren, U. *Anal. Chem.* **2002**, *74*, 199–202.  
 (24) Thiel, A. J.; Frutos, A. G.; Jordan, C. E.; Corn, R. M.; Smith, L. M. *Anal. Chem.* **1997**, *69*, 4948–4956.  
 (25) Lao, A. I. K.; Lee, T. M. H.; Hsing, I.-M.; Ip, N. Y. *Sens. Actuators, A* **2000**, *84*, 11–17.  
 (26) Lee, T. M.; Hsing, I. M.; Lao, A. I.; Carles, M. C. *Anal. Chem.* **2000**, *72*, 4242–4247.  
 (27) Poser, S.; Schulz, T.; Dillner, U.; Baier, V.; Köhler, J. M.; Schimkat, D.; Mayer, G.; Siebert, A. *Sens. Actuators, A* **1997**, *62*, 672–675.  
 (28) Northrup, M. A.; Ching, M. T.; White, R. M.; Watson, R. T. In *Technical Digest of Transducers '93, 7th International Conference on Solid State Sensors and Actuators*; Yokohama, Japan, 1993; pp 924–927.  
 (29) Northrup, M. A.; Gonzalez, C.; Hadley, D.; Hills, R. F.; Landre, P.; Lehew, S.; Saiki, R.; Sninsky, J. J.; Watson, R.; Watson, R. J. In *Technical Digest of the 8th International Conference on Solid-State Sensors and Actuators*; Middelhoeck, S., Cammann, K., Eds.; Stockholm, Sweden, 1995; Vol. 1, pp 764–767.  
 (30) Khandurina, J.; McKnight, T. E.; Jacobson, S. C.; Waters, L. C.; Foote, R. S.; Ramsey, J. M. *Anal. Chem.* **2000**, *72*, 2995–3000.  
 (31) Lagally, E. T.; Simpson, P. C.; Mathies, R. A. *Sens. Actuators, B* **2000**, *63*, 138–146.  
 (32) Zou, Q.; Miao, Y.; Chen, Y.; Sridhara, U.; Chong, C. S.; Chai, T.; Tieb, Y.; Teh, C. H. L.; Lim, T. M.; Heng, C. *Sens. Actuators, A* **2002**, *102*, 114–121.  
 (33) Lagally, E. T.; Emrich, C. A.; Mathies, R. A. *Lab Chip* **2001**, *1*, 102–107.  
 (34) Yamamoto, T.; Nojima, T.; Fujii, T. *Lab Chip* **2002**, *2*, 197–202.  
 (35) Swinney, K.; Bornhop, D. J. *Electrophoresis* **2001**, *22*, 2032–2036.  
 (36) Liu, J.; Enzelberger, M.; Quake, S. *Electrophoresis* **2002**, *23*, 1531–1536.

nucleic acid sequences.<sup>37–42</sup> They possess a hairpin-loop structure, with the “hairpin” consisting of a DNA double strand, with a fluorophore attached to the end of one strand and a molecule acting as a so-called “quencher” to the other. When the hairpin is closed (i.e., the DNA is hybridized in this portion of the molecule), the fluorophore and the quencher are close together, quenching possible fluorescence. A way of separating the double strand is to bring it to its  $T_m$ .<sup>37–39,41</sup> The  $T_m$  of the beacon’s double strand depends on its length and composition, and is very specific. When temperature is slowly increased, the double strand denatures progressively, and fluorescence increases as the fluorescent moiety is released from the quencher. By ramping up the temperature and measuring fluorescence, one obtains a melting curve from which it is possible to extract the  $T_m$  of a beacon. By using the specificity of the beacon melting curves, it is possible to precisely calibrate a microdevice with respect to temperature.

In this work, devices have been realized for use in solid-phase DNA hybridization-based analysis. An established oligonucleotide-immobilization technology that has proven to be relatively resistant to high temperatures<sup>43</sup> was transferred to microfluidic channels. The device was characterized thermally using a novel temperature calibration method based on molecular beacons. A simple and inexpensive vacuum-based flowing system was developed for reproducible surface modification. The use of this microfluidic device with integrated heaters for measurement of DNA melting curves was demonstrated.

## EXPERIMENTAL SECTION

**Device Fabrication.** A schematic of the device is shown in Figure 1. Each reactor chamber consists of a 2-cm-long straight channel, having widths of 500 or 1000  $\mu\text{m}$ , and etched to depths of 10 or 20  $\mu\text{m}$ , respectively, in a 500- $\mu\text{m}$ -thick, 10-cm-diameter Pyrex 7740 wafer. The reason for having such large channels was to have a large detection surface for heterogeneous assays. It was found that optical detection was best performed through an unstructured, 200- $\mu\text{m}$ -thick glass substrate when working with an inverted fluorescence microscope. Therefore, the bottom plate of the device, through which detection was performed, had to be transparent and could not have fluidic channels etched into it. The chambers were therefore etched into the top coverplate, which had predrilled access holes. A nonstandard photolithographic step was required, as it was impossible to create a uniform layer of photoresist on this wafer using a standard spin-coating process due to the presence of the access holes. First, a 400-nm-thick layer of polysilicon was deposited by low-pressure chemical vapor deposition in a furnace at 570  $^\circ\text{C}$  for 1 h. This was followed by a treatment with hexamethyldisilazane (HMDS) (Laporte Electronics, Riddings, U.K.) by exposure to HMDS vapor to increase adhesion of the photoresist to the polysilicon. A 6:4

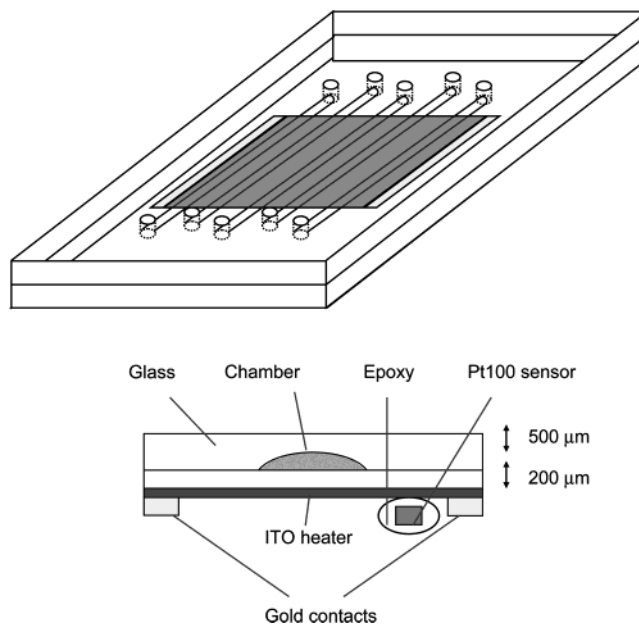


Figure 1. Schematic diagram of the device with chamber cross section. Overall dimensions are 23 mm (width)  $\times$  39 mm (length)  $\times$  0.7 mm (thickness). Diagram not to scale.

mixture of AZ4562 photoresist (Clariant GmbH, Switzerland)/propylene glycol methyl ether acetate (PGMEA) solvent (Aldrich, Switzerland) was then sprayed, rather than spin-coated, onto the substrate to obtain a 6- $\mu\text{m}$ -thick photoresist layer.

The resist layer was prebaked at 85  $^\circ\text{C}$  for 35 min in an oven, exposed, developed, and finally postbaked at 125  $^\circ\text{C}$  for 30 min, again in an oven. Pattern transfer and microchannel fabrication were performed as described previously.<sup>44</sup> The coverplate containing the access holes and the channels was sealed by fusion bonding to a 200- $\mu\text{m}$ -thick Pyrex 7740 wafer. The integrated heater consisted of a transparent, 50-nm-thick indium tin oxide (ITO) layer sputtered onto the bottom wafer, as previously reported (Kroll Thin Film Technologies, Neuchâtel, Switzerland).<sup>45,46</sup> Strips of 50-nm-thick chromium topped off by 150-nm-thick gold were evaporated along the sides of the ITO layer as electrical contacts to obtain a uniform electric field throughout the resistive heater. Scotch tape was used as a mask to spatially define the heater during deposition of the different resistive layers onto the device. A Pt100 platinum sensor (Minco, Aston, France) was glued to the ITO layer with thermally conductive, electrically insulating H70E EPO-TEK epoxy (Epoxy Technology, Switzerland) and cured at 100  $^\circ\text{C}$  in an oven to measure the temperature at this surface.

**Reagents.** Tris/HCl buffer (100 mM) containing 1 mM  $\text{MgCl}_2$  (pH 8) was made from tris(hydroxymethyl)aminomethane (Tris) (Fluka Chemicals, Buchs, Switzerland) and  $\text{MgCl}_2$  powder (Merck, Buchs, Switzerland) diluted in doubly distilled deionized (DI) water. NaOH solution (1 M; CE-grade, filtered over a 0.2- $\mu\text{m}$  membrane prior to packaging) was purchased from Fluka Chemi-

(37) Tyagi, S.; Kramer, F. R. *Nat. Biotechnol.* **1996**, *14*, 303–8.

(38) Tyagi, S.; Bratu, D. P.; Kramer, F. R. *Nat. Biotechnol.* **1998**, *16*, 49–53.

(39) Giesendorf, B. A.; Vet, J. A.; Tyagi, S.; Mensink, E. J.; Trijbels, F. J.; Blom, H. J. *Clin. Chem.* **1998**, *44*, 482–486.

(40) Bonnet, G.; Krichevsky, O.; Libchaber, A. *Proc. Natl. Acad. Sci. U.S.A.* **1998**, *95*, 8602–8606.

(41) Bonnet, G.; Tyagi, S.; Libchaber, A.; Kramer, F. R. *Proc. Natl. Acad. Sci. U.S.A.* **1999**, *96*, 6171–6176.

(42) Chen, W.; Martinez, G.; Mulchandani, A. *Anal. Biochem.* **2000**, *280*, 166–172.

(43) Adessi, C.; Matton, G.; Ayala, G.; Turcatti, G.; Mermod, J. J.; Mayer, P.; Kawashima, E. *Nucleic Acids Res.* **2000**, *28*, E87.

(44) Dodge, A.; Fluri, K.; Verpoorte, E.; de Rooij, N. F. *Anal. Chem.* **2001**, *73*, 3400–3409.

(45) Daridon, A.; Sequeira, M.; Pennarun-Thomas, G.; Dirac, H.; Krog, J. P.; Gravesen, P.; Lichtenberg, J.; Diamond, D.; Verpoorte, E.; de Rooij, N. F. *Sens. Actuators, B* **2001**, *76*, 235–243.

(46) Daridon, A.; Fascio, V.; Lichtenberg, J.; Wütrich, R.; Langen, H.; Verpoorte, E.; de Rooij, N. F. *Fresenius' J. Anal. Chem.* **2001**, *371*, 261–269.

cals, Buchs, Switzerland. H<sub>2</sub>SO<sub>4</sub> (97%; Merck, Buchs, Switzerland) was diluted to 50%. Electronic-grade ethanol, acetone, and 1 M HCl were purchased from Laporte Electronics (Riddings, U.K.). The acetone was dried over molecular sieves (400 Å mesh). Silanizing agent (3-aminopropyl)aminotriethoxysilane (ATS) was purchased from Aldrich (Buchs, Switzerland). Tris(2-carboxyethyl)phosphine hydrochloride (TCEP) and a heterobifunctional cross-linking reagent, *m*-maleimidobenzoyl-*N*-hydroxysulfosuccinimide ester (sulfo-MBS), were purchased from Pierce (Socochim SA, Switzerland). Phosphate-buffered saline (PBS) buffer (0.1 M NaH<sub>2</sub>PO<sub>4</sub>, 0.15 M NaCl, pH 7.2) and NaPi buffer (0.1 M NaH<sub>2</sub>PO<sub>4</sub>, 0.15 M NaCl, pH 6.5) were prepared from NaH<sub>2</sub>PO<sub>4</sub> (Merck, Buchs, Switzerland) and NaCl (Fluka, Buchs, Switzerland) powders dissolved in DI water and pH-adjusted with HCl. 5XSSC buffer (0.75 M NaCl, 0.075 M sodium citrate, pH 7.0) was prepared using chemicals from Fluka, Buchs, Switzerland. β-Mercaptoethanol (BME) was purchased from Sigma, Buchs, Switzerland. TMN stringent buffer is a solution of 10 mM Tris/HCl (pH 7.5) with 50 mM NaCl and 20 mM MgCl<sub>2</sub>.

**Oligonucleotides.** Cy5-Black Hole Quencher 3 (Cy5-BHQ3) beacon was purchased from Biosearch Tech, U.S.A. All the oligonucleotides were purchased from Eurogentec, Belgium. The sequences of the oligonucleotides used in the different experiments are given below.

(1) *Thiol Oligonucleotide Fluorescently Labeled with Texas Red (TR) (Used To Assess Thiol Oligonucleotide Binding to the Silane-Bound Cross-Linker)*. (T) 10-P2-TR: 5'-SH-TTTTTTTTTTGAG-GAAAGGGAAGGGAAAGGAAGG-TEXAS RED-3'

(2) *Oligonucleotides (Used in the Different Hybridization Experiments)*. (T) 10-P1 (surface-attached probe DNA with thiol group): 5'-SH-TTTTTTTTTTCACCAACCCAAACCAACCCAAACC-3'. TR-REV-P1 (target DNA in solution): 3'-GTGGTTGGGTTTG-GTTGGGTTTGG-Texas Red-5'. (T) 10-P2 (surface-attached probe DNA with thiol group): 5'-SH-TTTTTTTTTTGAGGAAAGGGAAGGAAAGGAAGG-3'. TR-REV-P2 (target DNA in solution): 3'-CTCCTTCCCTTCCCTTCCCTTCC-Texas Red-5'. (T) 10-P1 and TR-REV-P1 are complementary, as are (T) 10-P2 and TR-REV-P2.

**Instrumentation.** A homemade electronic circuit hooked up to a Hewlett-Packard power supply regulates the current flowing through the resistive ITO layer via a National Instruments (Austin, TX) DAQPad-6020 data acquisition board controlled by Labview PID software. A temperature control precision of ±0.5 °C was obtained with increasing temperature ramps of 10 °C/sec. Fluorescence images were taken with a CF 8/4 DXC black-and-white CCD camera (Kappa, Gleichen, Germany) mounted on an Axiovert S 100 fluorescence microscope equipped with a DC halogen lamp and a dichroic mirror set for Cy5 (excitation wavelength band-pass at 546 nm, dichroic mirror reflecting below 580 nm and transmitting above 590 nm) (Zeiss, Feldbach, Switzerland). Images were pixel-processed with Lispix freeware to obtain quantitative intensity data.

Experimental denaturation curves (melting curves) in solution assays for fluorescent beacons were generated in a Jasco FP 750 spectrofluorometer equipped with a temperature controller and stirring unit (Jasco ETC-272T). Excitation and emission wavelengths were fixed at 620 and 660 nm for Cy5. Oligonucleotides, diluted to a final concentration of 200 nM in 100 mM Tris/HCl containing 1 mM MgCl<sub>2</sub> (pH 7.8) buffer, were introduced into a

0.5 × 1.0-cm quartz cuvette (Hellma). Samples were stirred continuously with a magnetic bar during the measurements.

Denaturation curves of the P2 oligonucleotides were generated in a spectrophotometer (Jasco V550) equipped with a temperature controller (Jasco ETC-505T). Each pair of synthetic complementary oligonucleotides were diluted to a final concentration of 0.7 μM in 1 mL of buffer containing 100 mM Tris/HCl and 1 mM MgCl<sub>2</sub> (pH 8.0).

A flow system was used to remove dissociated DNA fragments (to prevent resettling) and bubbles created during experiments at elevated temperatures. This system consisted of a Harvard syringe pump (Harvard, U.K.) connected to PEEK tubing (o.d., 1.6 mm; i.d., 500 μm) (Upchurch, Switzerland). The tubes were interfaced to the chip with a PEEK plug designed in-house and fabricated at MECA (St-Aubin, Switzerland). These fittings were inserted into the coverplate holes, sealing well due to the elasticity of PEEK. The tubing was fixed snugly over the flanges of the plugs.

A manometer connected to the house vacuum with an exhaust valve to regulate the induced negative pressure was used to control the flow rates of conditioning solutions inside the microchambers.

**Temperature Calibration.** In this work, heating inside the device was accomplished using an ITO resistive heater on the bottom surface of the prototype. A voltage was applied across the layer to generate current and, in turn, Joule heat. Temperature was regulated using a Pt100 sensor glued to the ITO surface. Because this was an indirect means of monitoring temperature inside the microchannels, it was possible that the actual temperature inside a microchamber differed from the externally measured temperature, as observed by Yamamoto et al.<sup>34</sup> The method proposed in this work to calibrate temperature inside the microdevice used molecular beacons as temperature sensors. The molecular beacon chosen was a Cy5-BHQ3 beacon. Temperature calibration was performed by measuring the melting curve of the beacon at a concentration of 5 μM in a 100 mM Tris/HCl buffer containing 1 mM MgCl<sub>2</sub> (pH 8.0). This measurement was first performed in a conventional, precisely thermostated system by dipping a thermocouple inside the beacon solution, ramping the temperature up and measuring the fluorescence as the fluorescent moiety was released from the quencher. (Details of the instrumentation involved are given in the Instrumentation Section.) The beacon sample was then introduced into the device, and temperature was increased by heating with the ITO layer. Temperature was regulated by measuring temperature with the Pt100 sensor glued to the surface of the ITO layer. Images were taken using an inverted fluorescence microscope and a digital camera. Pixel processing of the images enabled generation of quantitative data, allowing calculation of the effect of temperature on fluorescence intensity. The resulting curve is sigmoidal in shape, with the *T<sub>m</sub>* being calculated by finding the inflection point of the fitted curve using Origin software. This point is found in the linear portion of the melting curve. The data in the linear range of beacon response obtained with external temperature measurement in the chip was correlated to that obtained in the conventional system to correct for differences in internal versus applied external temperature.

**Surface Conditioning Prior to Oligonucleotide Attachment.** Surface conditioning was performed by continuously

drawing conditioning fluids through the reaction chambers at constant controlled flow rates. Conventional methods for inducing controlled flows in microfluidic devices utilize peristaltic pumps or even more expensive devices, such as syringe pumps. In this work, a simple setup using house vacuum as a pumping mechanism was devised. When there is a difference of pressure,  $\Delta P$ , between the inlet and outlet of a channel, the flow induced in this channel can be obtained by

$$Q = \Delta P / R \quad (1)$$

where  $R$  is the channel fluidic resistance.<sup>47–49</sup> In this study, channels are much wider than they are deep and have profiles that can be approximated by a rectangle having a width much larger than the height.  $R$  is then given by<sup>47,48</sup>

$$R = 12\eta L / wh^3 \quad (2)$$

where  $\eta$  is the viscosity of the fluid in the channel,  $L$  is the length of the channel,  $w$  is the channel width, and  $h$  is the channel height.

Flow rate can then be calculated as

$$Q = wh^3 \Delta P / 12\eta L \quad (3)$$

From eq 3, it is clear that flow rates and, hence, reagent delivery to microchannel surfaces can be well-controlled, assuming a stable source of vacuum is available.

The surface modification procedure adopted here is based on that described in Adessi et al.<sup>43</sup> For all conditioning and reaction steps, solution was drawn through the chamber under constant flow conditions. Drops of each solution were placed over reservoir holes at one end of a chamber, and vacuum was applied to the other end. Chambers were first treated with bases and acids in order to always obtain the same starting surface conditions prior to silanization. The preconditioning sequence consisted of an initial 20-min rinse with 1 M NaOH, followed by a 10-min rinse with DI water. HCl (1 M), DI water, 50% H<sub>2</sub>SO<sub>4</sub>, and DI water were then sequentially flushed through the chamber for 10, 5, 20, and 5 min, respectively. A 5-min ethanol rinse removed excess water, followed by a 10-min rinse with dried acetone to remove ethanol. Silanization was then carried out by flushing with a solution of 1% ATS in dried acetone for 10 min. Dried acetone was used to rinse the solution away, followed by an ethanol rinse to prepare the chip for the next step (both rinses were 5 min long). For all conditioning steps, a negative pressure of  $7 \times 10^4$  Pa was applied to the 500- $\mu$ m-wide, 10- $\mu$ m-deep channels. This yields a flow rate of 8.4  $\mu$ L/min, assuming a  $\eta$  equivalent to that of water. Dividing the flow rate by the area of the channel cross section gives the average linear velocity, which was 28 mm/s in this case. For the 1000- $\mu$ m-wide, 20- $\mu$ m-deep channels,  $3 \times 10^4$  Pa was applied to generate a linear velocity of 48 mm/s.

A heterobifunctional reagent, sulfo-MBS, was used both as a spacer and as a cross-linker between the silane and the oligonucleotides. The sulfo-MBS is covalently attached to the amino silane through formation of an amide bond between the succinimidyl ester moiety of sulfo-MBS and amino groups of the silane. To carry out the reaction, a 5 mM solution of sulfo-MBS in PBS was flowed through the chamber for 10 min, followed by a 10-min PBS rinse, a 5-min DI water rinse, and finally, a 5-min ethanol rinse. This procedure was performed at linear velocities of 28 mm/s for the 500- $\mu$ m-wide chamber and 16 mm/s for the 1000- $\mu$ m-wide chamber. Concentration of the cross-linker solution had to be kept low in order to avoid nonuniform coatings and eventual clogging of the chamber due to precipitation, as observed previously for physisorption of protein A to a silanized microchannel surface.<sup>44</sup> The formation of microbubbles occurs on hydrophobic surfaces, and was observed here when the cross-linker reaction had more or less gone to completion, saturating the surface.

**Probe Immobilization.** The final step of the procedure for surface modification involved covalent attachment of the probe oligonucleotide via the thiol group on the 5' end to the maleimide portion of the sulfo-MBS cross-linker. The DNA probe molecules include a poly-T (T10) sequence to keep the sequences to be hybridized positioned away from the surface, as previously reported.<sup>43</sup> The binding step was followed by a 10-min rinse with NaPi buffer and a 10-min capping treatment using a solution containing 10 mM BME in NaPi solution to render all the remaining available cross-linker sites inactive. A 10-min rinse with NaPi buffer was performed to remove the BME, followed by a 5-min rinse with 5XSSC buffer, a solution in which DNA is stable and can be stored for longer periods of time when refrigerated.

In experiments to determine the densities of DNA bound to the spacer, a TR-labeled thiol oligonucleotide diluted in NaPi buffer, with 5 mM TCEP added to avoid thiol oxidation, was bound to the cross-linker. The fluorescence emitted by the TR label could then be used as a measure of probe molecule density.

The reproducibility of probe surface density in the 500- $\mu$ m-wide, 10- $\mu$ m-deep chambers was assessed by reacting 100  $\mu$ L of 1  $\mu$ M TR-labeled thiol oligonucleotide ((T)10-P2-TR) solution with the sulfo-MBS-modified surface. This was performed by drawing the solution through the chamber at a linear velocity of 12 mm/s for 30 min. Fluorescence images taken after rinsing away excess sample then allowed the reproducibility of the immobilization reaction to be determined.

Control of probe surface density was demonstrated by varying the reaction times of the oligonucleotide with cross-linker-treated surface. The DNA sequence used for these tests was the fluorescently labeled (T)-10-P2-TR. For the 1000- $\mu$ m-wide, 20- $\mu$ m-deep chambers, the flow rates of thiol oligonucleotide (probe molecules) required to achieve linear flow rates equivalent to the smaller chambers were significant, resulting in rapid consumption of reagent. Therefore, an alternative stopped-flow method was used to carry out oligonucleotide immobilization in this case. Probe-containing solution was introduced to a chamber with the controlled vacuum system at 8 mm/s. Once the chamber was filled, the flow was stopped in order to let passive diffusion of DNA to the surface take place for 1 min. This solution was then removed, and a second volume of probe solution drawn into the

(47) Kovacs, G. T. A. *Micromachined Transducers Sourcebook*; McGraw-Hill: New York, 1998; pp 792–793.

(48) Beebe, D. J.; Mensing, G. A.; Walker, G. M. *Ann. Rev. Biomed. Eng.* **2002**, *4*, 261–86.

(49) Shultz-Lockyear, L. L.; Colyer, C. L.; Fan, Z. H.; Roy, K. I.; Harrison, D. J. *Electrophoresis* **1999**, *20*, 529–538.

chamber for a 1-min stopped-flow reaction, and so on. The total effective reaction time increased with the number of times the solution replenishment process was performed.

**Hybridization/Dehybridization Experiments.** For hybridization tests, the nonlabeled thiol oligonucleotides, (T) 10-P1 and (T) 10-P2, diluted in the same buffer solution as the labeled thiol oligonucleotide, were bound to cross-linker-treated chambers. Reaction times were kept constant at 30 min. Surface densities of the bound probe DNA were determined by hybridizing with a fluorescent complementary oligonucleotide, either TR-REV-P1 or TR-REV-P2, depending on the experiment. All complementary oligonucleotides were prepared in 5XSSC buffer at a 100 nM concentration and hybridized in both the small and large chambers using the stopped-flow technique described above. Surface densities of hybridized oligonucleotides could be actively controlled by either varying the concentration of thiol oligonucleotides in the solutions for the immobilization reaction or by varying incubation times of the fluorescent complementary oligonucleotides.

The degree of hybridization versus nonspecific adsorption was determined by measuring the difference in signal-to-noise ratios for binding between surface-immobilized (T) 10-P1 and its complementary strand, TR-REV-P1, versus binding with the noncomplementary TR-REV-P2. Probe immobilization reactions were performed for 30 min. Hybridization experiments were carried out using solutions containing 100 nM of the two target DNA species in either 5XSSC buffer or TMN stringency buffer. The duration of the incubation periods for hybridization was 30 min.

Melting curves of surface-bound double strands were obtained using a continuous flow technique. The (T) 10-P2 and TR-REV-P2 complementary pair was used. The probe DNA was first immobilized in a 1000- $\mu\text{m}$ -wide, 20- $\mu\text{m}$ -deep chamber using a 30-min reaction time. Target DNA was then incubated with the probes for another 30 min. A 5  $\mu\text{L}/\text{min}$  flow of 5XSSC buffer was continuously pumped through a fully conditioned chamber with the Harvard syringe pump connected to the PEEK interface. Temperature was slowly ramped up at a rate of 1  $^{\circ}\text{C}/\text{s}$  with the ITO resistive heater and stabilized every 5 $^{\circ}$  for 5 s in order to take a snapshot of the fluorescence image with the CCD camera mounted on the fluorescence microscope. As temperature increased, dehybridization occurred, releasing hybridized, labeled strands, which were continuously removed in the applied flow. A decrease in fluorescence signal at the surface was therefore observed.  $T_m$ 's of the melting curves obtained were determined by first fitting them with a sigmoidal function and then calculating the inflection points of the fitted curves, as was done with the beacon. Melting curves were also measured in a conventional system in the liquid phase to compare with the results obtained for solid-phase hybridization.

## RESULTS AND DISCUSSION

**Temperature Calibration.** The internal temperature inside the device needed to be calibrated as a function of the externally applied temperature at the ITO layer to ensure optimum DNA hybridization–dehybridization conditions. This was done by recording the fluorescence-versus-temperature melting curves for the Cy5-BHQ3 beacon in both a conventional (reference) system and the microfluidic device. The  $T_m$  of the beacon was always

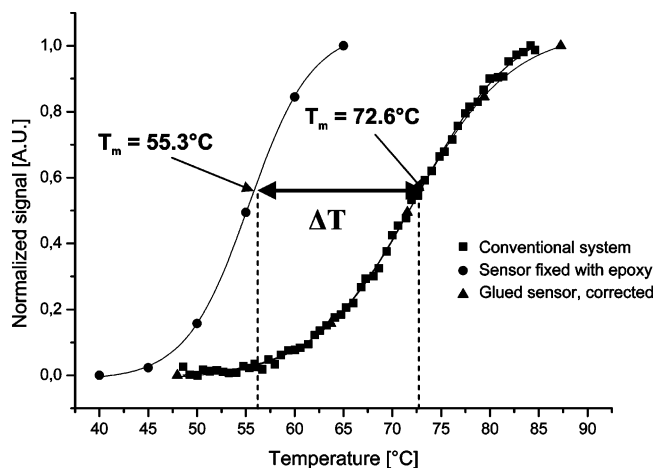


Figure 2. Different normalized melting curves for Cy5-BHQ3 beacon. Curves corresponding to the conventional  $T_m$  determination method and the calibrated glued-sensor method match well. Beacon concentration: 5  $\mu\text{M}$  in 100 mM Tris/HCl buffer containing 1 mM  $\text{MgCl}_2$  (pH 8.0) for all measurements.

determined using melting curves normalized to the maximum value of fluorescence recorded. The beacon yielded a  $T_m$  of 72.6  $^{\circ}\text{C} \pm 0.4$   $^{\circ}\text{C}$  ( $n = 3$ ) in the conventional system versus 55.3  $^{\circ}\text{C} \pm 0.3$   $^{\circ}\text{C}$  ( $n = 3$ ) in the chip, which gives an apparent temperature shift,  $\Delta T$ , of 17.3  $^{\circ}\text{C}$ . The melting curves are presented in Figure 2. The measurements indicated by the squares (■) correspond to signal measured in a conventional system, while the circles (●) represent the measurements performed in the microdevice. The two curves are very similar in shape, regardless of the strong shift along the temperature axis. The curve measured in the conventional system is a reliable reference, since the instrument was well-thermostated, and temperature was measured directly in the beacon solution by immersing a thermocouple into the cuvette. Hence, the measured external temperature applied at the ITO layer is clearly lower than the actual temperature inside the microchannel. Such artifacts can be corrected for by calibrating devices with respect to temperature using molecular beacons as temperature probes. In this case, the temperature difference was caused by the epoxy, used to glue the Pt100 sensor to the ITO heating layer, being a poor thermal conductor.

To perform the establishment of a reliable relationship between the external temperature measured with the Pt100 sensor in epoxy,  $T_{\text{ext}}$ , and actual temperature inside the channel,  $T_{\text{int}}$ , the linear regions of the Cy5-BHQ3 melting curves obtained in conventional and microchip systems were compared. The differences in internal versus external temperature,  $\Delta T (= T_{\text{int}} - T_{\text{ext}})$ , were calculated for each normalized fluorescence value that fell within the linear regions of both curves. (The difference in  $T_m$  was measured in the same way (Figure 2).) For the microchip curve, the linear region extended between 47 and 57  $^{\circ}\text{C}$ . In the conventional case, the linear region fell in the range 60–75  $^{\circ}\text{C}$ . The  $\Delta T$  values were then plotted as a function of  $T_{\text{ext}}$ , as shown in Figure 3. This plot is linear and indicates that  $\Delta T$  in fact increases with increasing applied external temperature. Moreover,  $\Delta T$  is 0 at  $\sim 26$   $^{\circ}\text{C}$ , which is close to room temperature. Yamamoto et al. also observed a linear relationship between  $T_{\text{ext}}$  and  $T_{\text{int}}$  for a PDMS microreactor array in contact with a thin-layer heater device.<sup>34</sup>

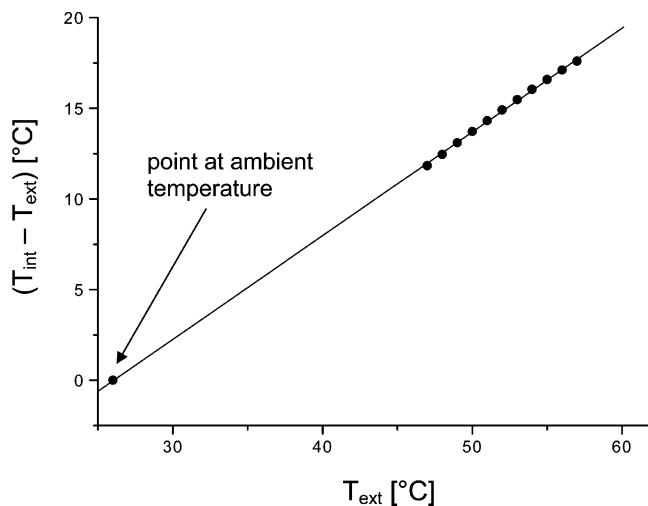


Figure 3. Difference in temperature,  $\Delta T = T_{\text{int}} - T_{\text{ext}}$ , between actual temperature inside the microchannel ( $T_{\text{int}}$ ) and external temperature measured with the Pt100 sensor ( $T_{\text{ext}}$ ), plotted as a function of  $T_{\text{ext}}$ .  $\Delta T$  was calculated using the linear regions of the Cy5-BHQ3 melting curves obtained in conventional and microchip systems, as explained in the text. The good linearity of this curve means that a reliable model exists for extracting  $T_{\text{int}}$  inside a microchannel from  $T_{\text{ext}}$ , measured with the Pt100 sensor.

Hence, the experimentally obtained  $\Delta T(T_{\text{ext}})$  plot can be used to correct the temperature axis of the Cy5-BHQ3 melting curve obtained using the Pt100 sensor embedded in epoxy so that this axis represents actual temperature inside the microchambers. A line was fitted by linear regression to the measured data points in Figure 3 to yield the following equation:

$$T_{\text{int}} = 1.57T_{\text{ext}} - 14.9 \quad (4)$$

The corrected melting curve for the glued-sensor measurement is also given in Figure 2 ( $\blacktriangle$ ), and agrees well with that obtained in the conventional fluorometer under controlled thermostated conditions. In this way, the determinate error introduced by the poor thermal contact between the Pt100 sensor and the ITO layer could be corrected. This method represents a novel technique to noninvasively and precisely calibrate the internal temperature of a transparent microfluidic device.

**Surface Conditioning.** Using the controlled reagent delivery system in conjunction with the 500- $\mu\text{m}$ -wide, 10- $\mu\text{m}$ -deep structures, a reproducibility of 9% ( $n = 3$ ) was obtained for immobilization of oligonucleotides. This was better than the 20% obtained on microscope slides.<sup>43</sup> The remaining error can probably be explained by the fact that the precision of the manometer used in the setup was only  $\pm 0.5 \times 10^4$  bar, resulting in a flow rate error of  $\pm 0.3 \mu\text{L}/\text{min}$  for the 10- $\mu\text{m}$ -deep channel. Since flow rates range between 3.6 and 8.4  $\mu\text{L}/\text{min}$  in the small channel, values for flow rate precision fall between 8 and 4%, respectively. Using a high-precision peristaltic pump or a syringe pump with nanoliter-per-minute flow precision, even better surface conditioning reproducibility could be expected. Nevertheless, this simple and nonexpensive system manages to achieve good reproducibility with fast reaction times, with a total procedure time of  $\sim 4$  h. This is much faster than the 2 days required in the original publication, in which this DNA immobilization method was applied to glass

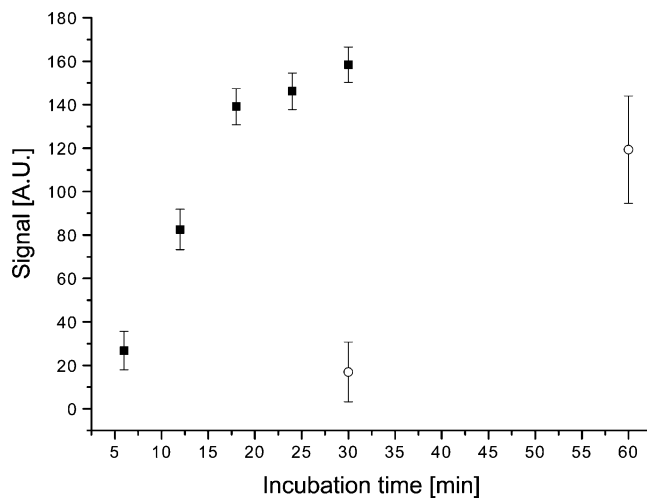


Figure 4. Binding of labeled probe thiol oligonucleotide to cross-linker-treated surface in a 1000- $\mu\text{m}$ -wide, 20- $\mu\text{m}$ -deep device. A stopped-flow reaction technique was used in this case. Signal ( $\blacksquare$ ) increases with reaction time until all cross-linker sites are saturated for the 1-min reaction/refill case, as expected. DNA solution depletes in  $< 1$  min, since signal ( $\circ$ ) does not increase when reaction times of 5 min per refill are used. Standard deviations of single measurements obtained by pixel processing of a surface image are dependent on the uniformity of the conditioned surface. [(T) 10-P2-TR] was 1  $\mu\text{M}$  in 5XSSC buffer with 5 mM TCEP.

slides.<sup>43</sup> It should be noted, however, that reaction times have not been optimized in either the slide or microchannel case, and improvements should be achievable in both cases. The advantage that microfluidic devices offer over glass slides is controlled convective transport of reagents over the surface being modified.

In the 1000- $\mu\text{m}$ -wide, 20- $\mu\text{m}$ -deep chamber, a stopped-flow reaction technique was used to conserve DNA reagent, as described in the Experimental Section. In the standard case, reagent solution was left to react for 1 min in the chamber before being refilled by fresh reagent. Total reaction time is then simply the product of the number of refill cycles and the reaction time per cycle. It was possible to vary the density of TR-labeled probe DNA bound to the surface, as evidenced in Figure 4. For 1-min reaction times, the surface concentration of TR-DNA approached its maximum after 20 refill cycles, indicating that cross-linker sites available for binding were close to being fully occupied. A simple test proved that it was not necessary to wait longer than 1 min between chamber refills. Reaction times of 5 min/cycle resulted in a lower fluorescence signal after a total time of 30 min than in the 1 min/cycle case. In fact, the signal was more-or-less equivalent to that obtained for 1-min times for the same number (6) of refills. The result at 60-min total reaction time, obtained after 12 5-min refill cycles, is also lower than after 30 min in the 1 min/cycle case. This indicates that the reagent solution was rapidly depleted so that reaction rates at the end of the 1-min and 5-min incubation periods were very small and about the same.

For testing specificity of hybridization in the microchannels, the nonfluorescent thiol oligonucleotide (T) 10-P1 was bound to the surface, and a hybridization experiment was performed first with the unrelated labeled target, TR-REV-P2, to measure the mishybridization signal. Stopped-flow conditions were used. The chamber was reinitialized by performing a 20-min NaOH (1 M) rinse to remove the immobilized DNA, followed by reconditioning

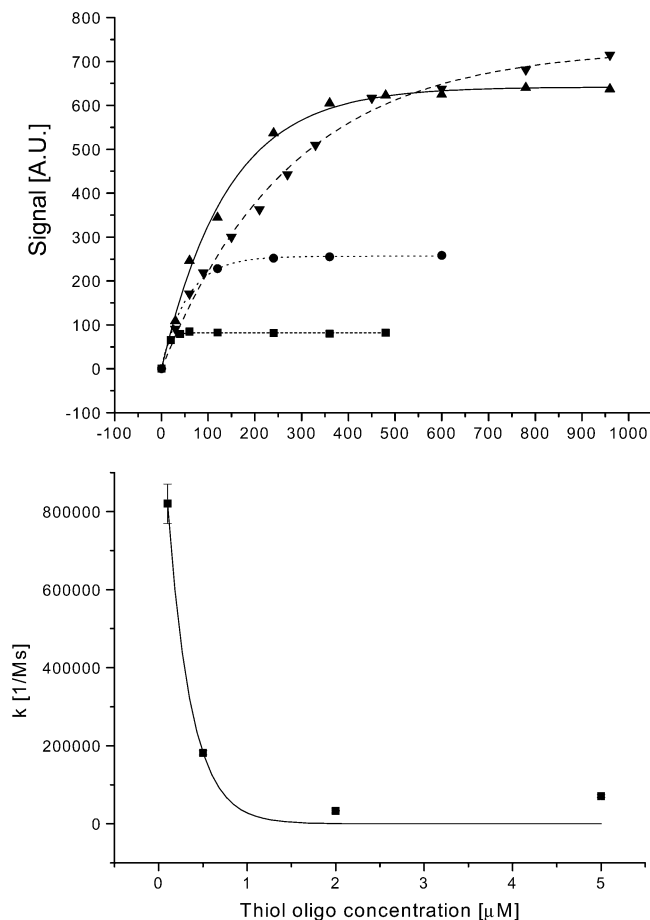


Figure 5. (a) Variation of T (10) P2-SH thiol oligonucleotide concentration in the reagent solution for surface immobilization induces variation of surface density. T (10) P2-SH solution concentrations: ▲, 5.0  $\mu\text{M}$ ; ▼, 2.0  $\mu\text{M}$ ; ●, 0.5  $\mu\text{M}$ ; ■, 0.1  $\mu\text{M}$ . These experiments were performed in a 500- $\mu\text{m}$ -wide, 10- $\mu\text{m}$ -deep chamber. Bound oligonucleotide density is revealed by hybridization with the fluorescently labeled complementary oligonucleotide. Signal increases until saturation of all available hybridization sites. Saturation signal increases with surface-bound DNA density. (b) On the other hand, forward rate constants for hybridization decrease because surface-bound DNA probe molecules are packed closer together, therefore reducing spatial freedom. [TR-REV-P2] = 100 nM.

with (T) 10-P1. A solution containing the complementary probe, TR-REV-P1, was then introduced and allowed to react with the surface. Hybridization of complementary oligonucleotides produces a strong difference in signal when compared to mismatched hybridization of unrelated probes. A signal-to-noise ratio of  $9.6 \pm 23\%$  for specific hybridization versus  $3.5 \pm 19\%$  ( $n = 3$  in both cases) was obtained for mismatched hybridization when experiments are performed with the 5XSSC buffer (results not shown). In this case, the specific/nonspecific binding signal ratio was 2.7. Sufficiently stringent surface hybridization conditions, here attained with the TMN buffer, lead to good hybridization specificity for complementary versus unrelated DNA strands. The signal-to-noise ratio decreases to 6.0, but the specific/nonspecific binding signal ratio is 6.0, which is 2.2-fold better than that obtained with the 5XSSC buffer (results not shown).

By varying incubation times of complementary target DNA, it was possible to control their surface densities, as seen in Figure 5a. Signal increases until all available bound probe DNA sites are

saturated. In addition, by varying the concentration of probe thiol oligonucleotides in the reagent solution but keeping reaction times fixed, it is possible to control surface densities of the covalently bound probe DNA. The maximum signal due to hybridized, fluorescently labeled complementary probes increases as a function of the concentration of thiol oligo in the original solution used for immobilization. These curves are typical for binding experiments from which kinetic data can be extracted. The kinetics of DNA hybridization to surface-tethered probes is a subject of ongoing investigation in a number of research groups, with second-order (bimolecular) or modified Langmuir adsorption models being proposed.<sup>50–52</sup> In our system, a second-order model neglecting the reverse (dehybridization) reaction was chosen. The rate equation is given in eq 4,

$$S(t) = S_0(1 - e^{-k[L]t}) \quad (5)$$

where  $S(t)$  is the number of bound molecules,  $S_0$  is the total number of available binding sites,  $k$  is the forward hybridization rate constant,  $[L]$  is the concentration of sample in solution, and  $t$  is the incubation time.

By fitting the binding curves using this function, the forward rate constant,  $k$ , can be deduced. As Figure 5a shows, agreement of the fitted curves with experimental data is good, indicating that our kinetic model is appropriate. The four forward rate constants obtained for the curves in Figure 5a and plotted in Figure 5b reveal an interesting point. For the lowest surface density of probe DNA, obtained using a reagent solution of 0.1  $\mu\text{M}$  concentration,  $k_{0.1} = 820\,000 \text{ M}^{-1} \text{ s}^{-1}$ . For the highest surface density,  $k_{5.0} = 71\,000 \text{ M}^{-1} \text{ s}^{-1}$ , which is indicative of a decrease in reaction rate of 91%. This decrease could be due to the fact that the immobilized oligonucleotides are closer to each other when surface densities increase, thereby reducing the spatial freedom that is necessary for hybridization enhancement.<sup>53,54</sup> Hybridization rate is quite sensitive to surface density of bound DNA, as indicated by the exponential decrease of forward rate constant versus primer concentration depicted in Figure 5b. From the saturation values of each curve in Figure 5a, the dose–response curve in Figure 6 was obtained, with “dose” being the density of DNA immobilized on the surface (designated here as “thiol oligo concentration”). The saturation signal increases up to a certain point and then decreases again with increasing attached oligonucleotide density. This again could be due to the fact that hybridization is inhibited when oligonucleotides are too close to each other.<sup>53,54</sup> Shchepinov et al. showed that hybridization yields are enhanced when surface-bound DNA molecules are given more spatial freedom to interact with DNA molecules in solution.<sup>53</sup> The use of so-called spacer molecules to increase the distance between the bound DNA and the solid substrate, thereby reducing steric hindrance, is one of

(50) Okahata, Y.; Kawase, M.; Niikura, K.; Ohtake, F.; Furusawa, H.; Ebara, Y. *Anal. Chem.* **1998**, *70*, 1288–1296.

(51) Cantor, C. R.; Smith, C. L. *Genomics*; John Wiley & Sons: New York, 1999; pp 89–90.

(52) Georgiadis, R.; Peterlinz, K. P.; Peterson, A. W. *J. Am. Chem. Soc.* **2000**, *122*, 3166–3173.

(53) Shchepinov, M. S.; Case-Green, S. C.; Southern, E. M. *Nucleic Acids Res.* **1997**, *25*, 1155–1161.

(54) Peterson, A. W.; Heaton, R. J.; Georgiadis, R. M. *Nucleic Acids Res.* **2001**, *29*, 5163–5168.

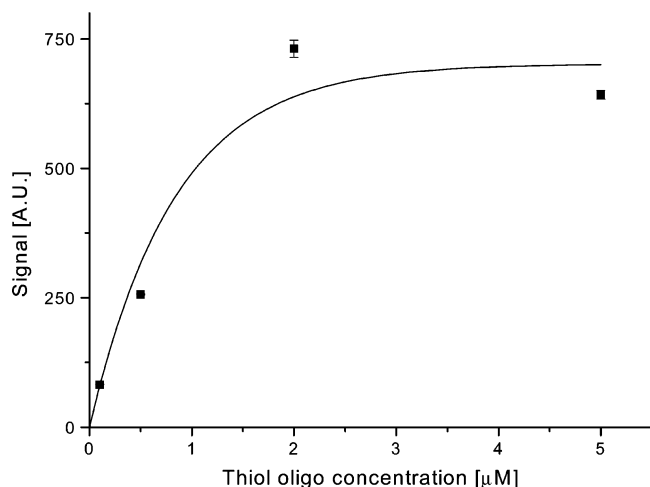


Figure 6. Dose–response curve, with the “dose” in this case being surface density. These points are the saturation signals from the curves in Figure 5a. Signal increases as a function of the concentration of thiol oligonucleotide reagent used for immobilization until saturation. A slight signal decrease was observed at the highest reagent concentration, due to spatial restriction of bound oligonucleotides leading to inhibited hybridization. Curve for sake of clarity.

the ways to accomplish this. Fluorescence quenching may also play a role, as a result of the close proximity of fluorophores in the more compact environment of densely packed hybridized oligonucleotides.

This type of study makes it possible to optimize surface densities in order to obtain a good compromise between hybridization signal and rate of hybridization. The different tests described above show that there is a large degree of flexibility and excellent control of surface definition possible within a microfluidic system. This is due to the enhanced control of solution transport provided by microfluidic devices, a feature which is difficult to obtain in macroscopic systems.

**Thermal Stability of the Covalently Bound DNA Probe Layer.** To test stability of the modified surface with respect to heat, (T) 10-P2-TR was bound to the conditioned surface in the larger chamber. Temperature was thermocycled according to a PCR protocol under conditions of continuous buffer flow. The surface was subjected to long heat treatments, with each cycle consisting of stages of 95 °C for 30 s, 60 °C for 5 min, and 72 °C for 7 min. As Figure 7 shows, a 30% drop in the signal due to labeled, bound DNA was observed during the first cycle, and a total drop of 78% was recorded over 25 cycles. This suggests a strong instability of the chemically modified surface when subjected to these extreme conditions. Chemical bond strength considerations lead to the conclusion that the silane bonds are the ones to break when energy is introduced to the system. For cycling conditions in which the times are reduced to 30, 90, and 90 s for temperatures of 95, 60, and 72 °C, respectively, the signal drop is ~40% for 40 cycles (data not shown). Photobleaching was measured in a separate experiment, and a drop of 16.3% in signal was observed after 10 min of exposure. For the total exposure time of 40 s for this experiment, the decrease in signal corresponding to bleaching was only 3%. Therefore, the contribution of photobleaching in these experiments is negligible. Because the curve in Figure 7 is reproducible, it could be fit with an

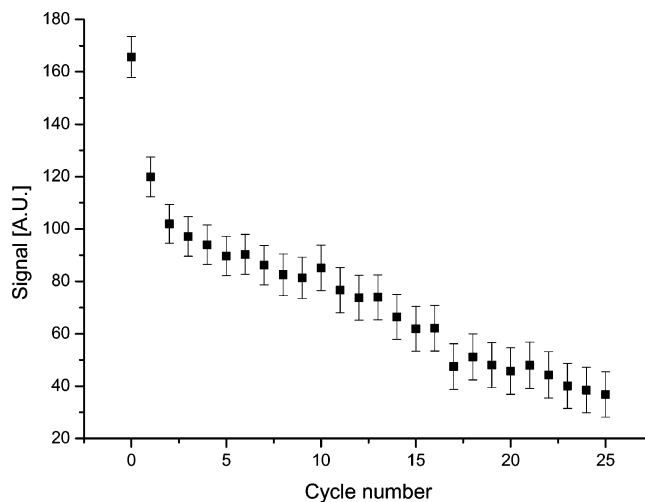


Figure 7. Decrease of surface-bound probe density as a function of thermocycle number. The (T) 10-P2-TR primer was used in this experiment. A decrease of 30% is observed after the first cycle, revealing instability of surface conditioning with respect to elevated temperature. The curve is reproducible, which could allow for signal intensity correction if quantitative analysis is desired.

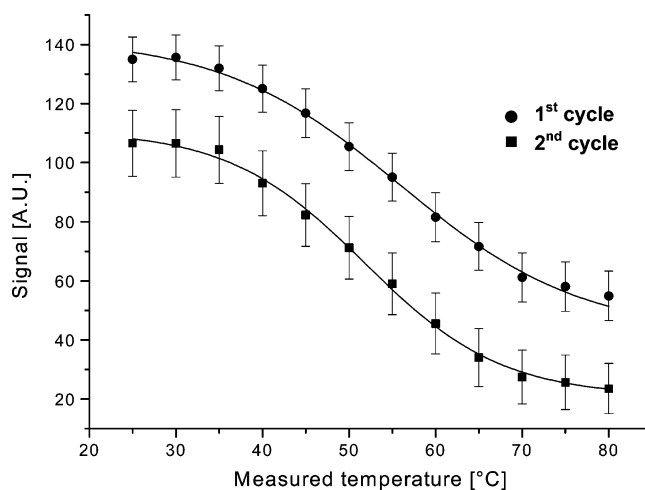


Figure 8. Two consecutive melting curve measurements for hybridized T(10) P2/TR-REV-P2. The initial signal decrease of 20% can be explained by surface instability with respect to heat. The  $T_m$ 's deduced from the curves nevertheless remain the same. A constant buffer flow of 5  $\mu\text{L}/\text{min}$  was applied to remove dehybridizing strands. Temperature was ramped up in steps of 5 °C, and images were acquired with a fluorescence microscope when temperature had stabilized after 5 s. [T(10) P2] in 5xSSC buffer with 5 mM TCEP added was 1  $\mu\text{M}$ , [TR-REV-P2] in 5xSSC buffer was 100 nM.

exponentially decreasing function and used to correct intensity values after each cycle for quantitative analysis.<sup>55</sup>

Dehybridization with the flow setup gave a measured  $T_m$  for the (T) 10-P2/TR-REV-P2 system of 56.2 °C  $\pm$  0.9 °C ( $n = 5$ ) for the first cycle (Figure 8). Correcting for  $T_{\text{ext}}$  using eq 3, a  $T_{\text{int}}$  of 73.4 °C  $\pm$  0.9 °C was obtained. This is close to the value obtained in the conventional system,  $T_{\text{mP2liquid}} = 74.4$  °C  $\pm$  0.4 °C ( $n = 4$ ). After a first thermal cycle, the system was rehybridized and thermally dehybridized again. The curve for the second cycle in Figure 8 gives the same  $T_m$ , but the total intensity has decreased

(55) Abel, A. P.; Weller, M. G.; Duveneck, G. L.; Ehrat, M.; Widmer, H. M. *Anal. Chem.* **1996**, *68*, 2905–12.

by 20%. The total measurement precision of  $\pm 1$  °C for  $T_m$  and the reproducibility of curve shapes should enable SNP analysis with this device.<sup>21,22</sup>

#### CONCLUSIONS

A microfluidic system with surface-bound DNA has been fully characterized in terms of thermal control and surface modification. A novel noninvasive technique for thermal calibration inside a microchannel has been developed and exploited using molecular beacons as temperature probes. Surface treatments are reproducible and highly controllable in a microfluidic channel, and surface-conditioning times are strongly reduced. Kinetic data can be extracted from binding curves in order to optimize surface densities for optimal reaction times. A novel way of performing thermal dehybridization has successfully been used to determine melting temperature measurements of strands of DNA. Taken together, this combined microfluidic/small-volume heating ap-

proach represents a powerful tool for surface-based DNA analysis and could be implemented effectively in applications such as SNP analysis.

#### ACKNOWLEDGMENT

The authors wish to thank Jan Lichtenberg (de Rooij Group, IMT) for helpful discussions in developing the heating interface, and Cédric Bucher (Shah Group, IMT) for the ITO depositions. P. Mayer (Manteia S.A.) is also thanked for helpful discussions. This work was supported by the Swiss Commission for Technology and Innovation program MedTech, Project No. 572.

Received for review April 12, 2003. Accepted December 22, 2003.

AC034377+